

A Fourier Finite-Element Method in a Non-Orthogonal System of Coordinates for the Simulation of 3D Resistivity Measurements Acquired in Petroleum Engineering

D. Pardo, M. J. Nam, C. Torres-Verdín, V. Calo

Basque Center for Applied Mathematics (BCAM)

TEAM MEMBERS:

*D. Pardo (Research Professor)
I. Garay (Postdoctoral Fellow)
I. Andonegui (Technician)*

MAIN COLLABORATORS:

*M. J. Nam, F. de la Hoz
M. Paszynski, L.E. García-Castillo
I. Gómez, C. Torres-Verdín*

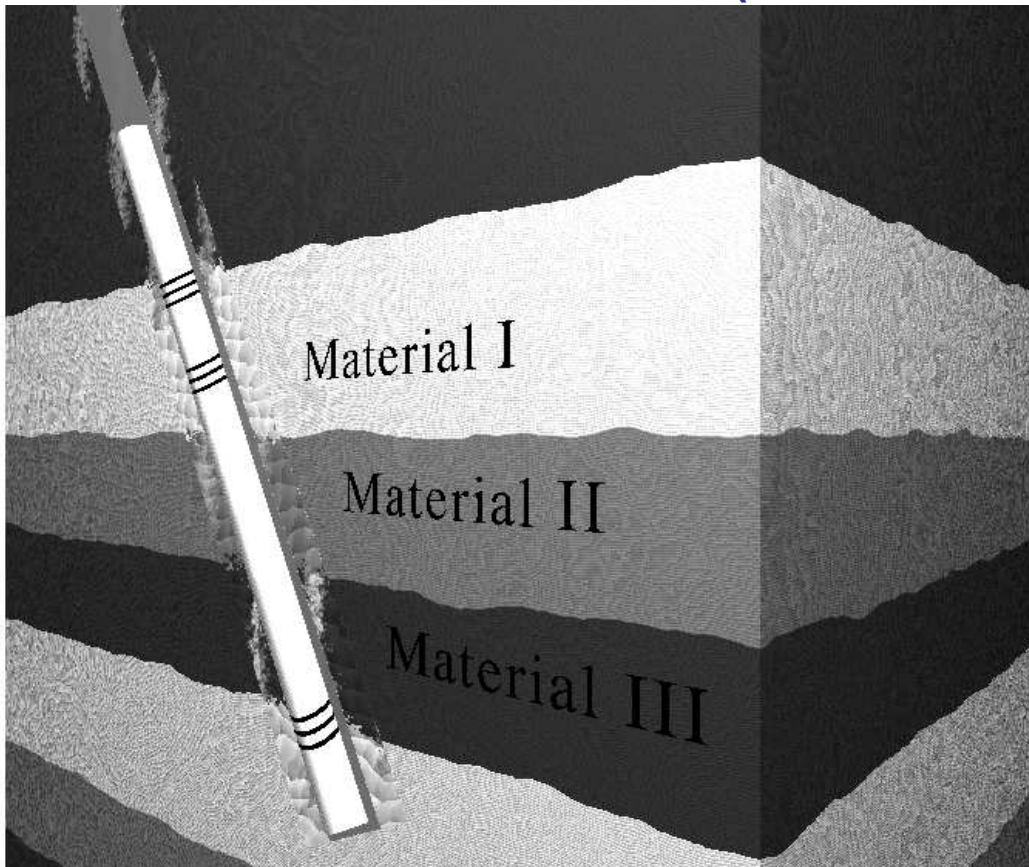
July 17th, 2009

Overview

- 1. Motivation and Objectives: Petroleum Engineering Electromagnetic Applications.**
- 2. Method:**
 - Fourier hp -Finite Element Method
 - Self-Adaptive Goal-Oriented hp Adaptivity.
- 3. Numerical Results.**
 - Induction logging.
 - Marine Controlled Source Electromagnetic (CSEM) Measurements.
- 4. Conclusions.**

motivation and objectives

Deviated Wells (Forward Problem)



Dip Angle

Invasion

Anisotropy

Different Sources
(Triaxial Induction)

Eccentric Logging
Instruments

Laterolog

Through-Casing

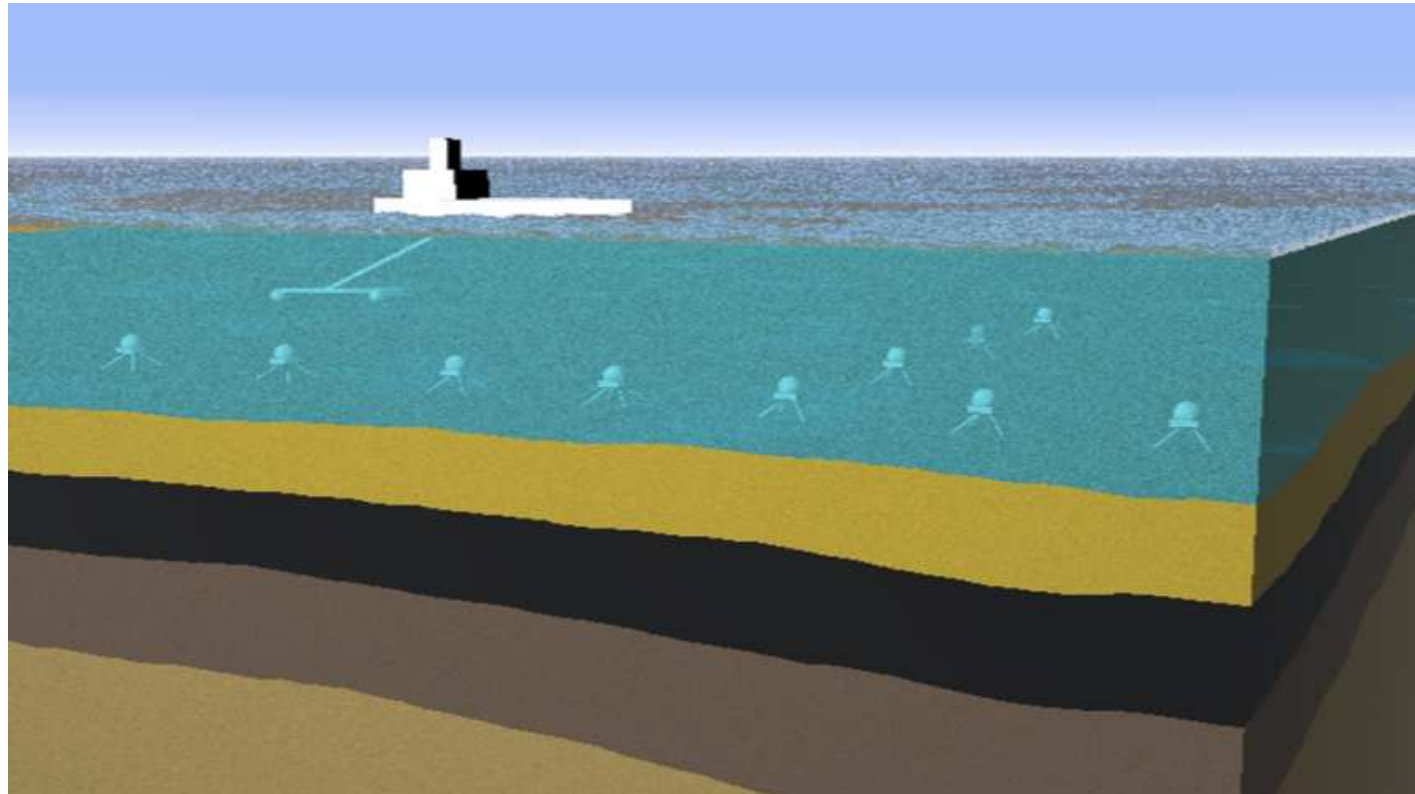
Induction-LWD

Induction-Wireline

Goal: To find the EM fields at the receiver antennas.

motivation and objectives

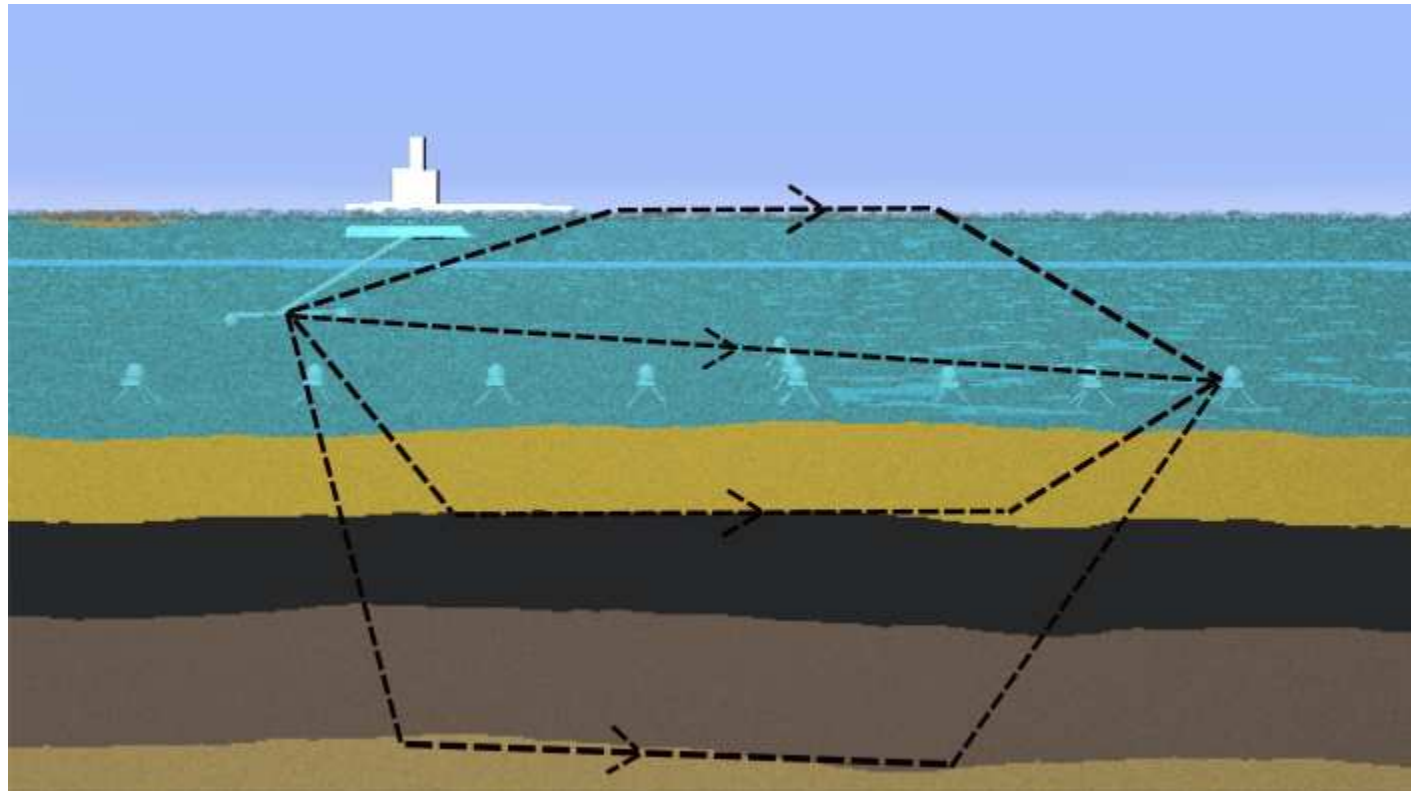
Marine Controlled Source Electromagnetics (CSEM)



Marine CSEM Measurements Acquisition System

motivation and objectives

Marine Controlled Source Electromagnetics (CSEM)



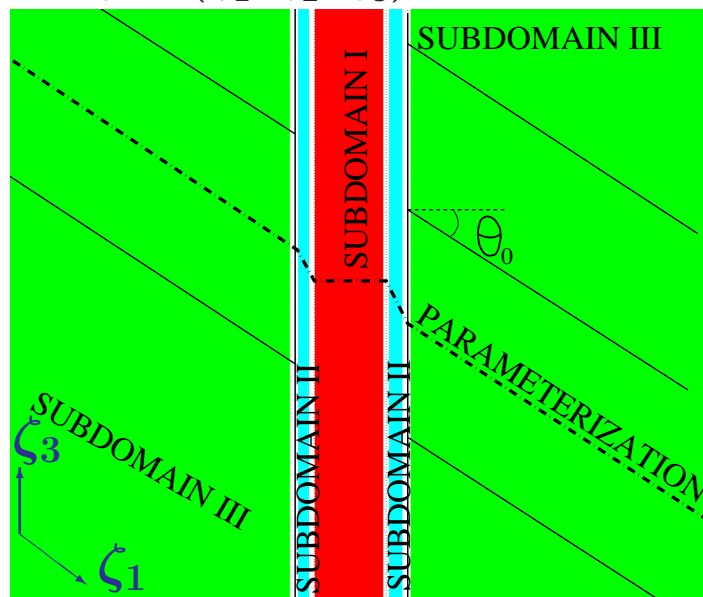
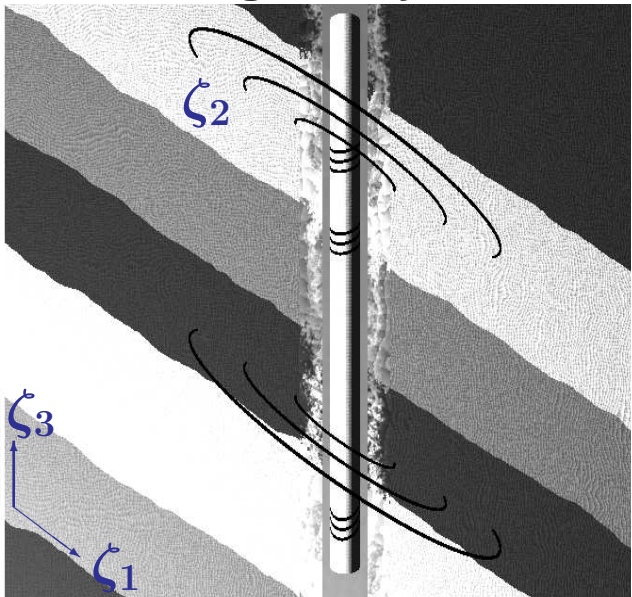
EM waves travelling through the air, sea, and sub-surface.



Fourier series expansion

Cartesian system of coordinates: $x = (x, y, z)$.

New non-orthogonal system of coordinates: $\zeta = (\zeta_1, \zeta_2, \zeta_3)$.



Subdomain I

$$\begin{cases} x = \zeta_1 \cos \zeta_2 \\ y = \zeta_1 \sin \zeta_2 \\ z = \zeta_3 \end{cases}$$

;

Subdomain II

$$\begin{cases} x = \zeta_1 \cos \zeta_2 \\ y = \zeta_1 \sin \zeta_2 \\ z = \zeta_3 + \tan \theta_0 \frac{\zeta_1 - \rho_1}{\rho_2 - \rho_1} \rho_2 \end{cases}$$

;

Subdomain III

$$\begin{cases} x = \zeta_1 \cos \zeta_2 \\ y = \zeta_1 \sin \zeta_2 \\ z = \zeta_3 + \tan \theta_0 \zeta_1 \end{cases}$$

Fourier series expansion

Variational Formulation in the New System of Coordinates

We define the Jacobian matrix of the change of coordinates $\mathcal{J} = \frac{\partial(x_1, x_2, x_3)}{\partial(\zeta_1, \zeta_2, \zeta_3)}$ and its determinant $|\mathcal{J}| = \det(\mathcal{J})$.

Variational formulation in the new system of coordinates:

$$\left\{ \begin{array}{l} \text{Find } u \in u_D + H_D^1(\Omega) \text{ such that:} \\ \left\langle \frac{\partial v}{\partial \zeta}, \tilde{\sigma} \frac{\partial u}{\partial \zeta} \right\rangle_{L^2(\Omega)} = \langle v, \tilde{f} \rangle_{L^2(\Omega)} \quad \forall v \in H_D^1(\Omega), \end{array} \right.$$

where:

$$\tilde{\sigma} := \mathcal{J}^{-1} \sigma \mathcal{J}^{-1T} |\mathcal{J}| \quad ; \quad \tilde{f} := f |\mathcal{J}| .$$

Same variational formulation with new materials and load data

Fourier series expansion

For a mono-modal test function $v = v_k e^{jk\zeta_2}$, we have:

$$\left\{ \begin{array}{l} \text{Find } u \in u_D + H_D^1(\Omega) \text{ such that:} \\ \\ \sum_{m,n} \left\langle \left(\frac{\partial v}{\partial \zeta} \right)_k e^{jk\zeta_2}, \tilde{\sigma}_m \left(\frac{\partial u}{\partial \zeta} \right)_n e^{j(m+n)\zeta_2} \right\rangle_{L^2(\Omega)} = \\ = \sum_l \left\langle v_k e^{jk\zeta_2}, \tilde{f}_l e^{jl\zeta_2} \right\rangle_{L^2(\Omega)} \quad \forall v_k e^{jk\zeta_2} \in H_D^1(\Omega) \end{array} \right.$$

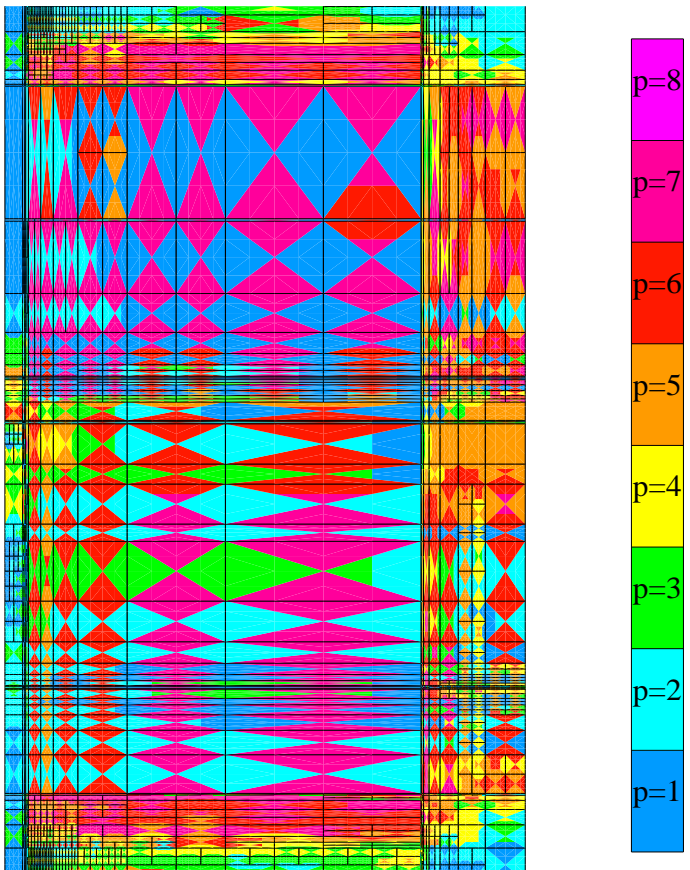
Using the L^2 -orthogonality of Fourier modes:

$$\left\{ \begin{array}{l} \text{Find } u \in u_D + H_D^1(\Omega) \text{ such that:} \\ \\ \sum_n \left\langle \left(\frac{\partial v}{\partial \zeta} \right)_k, \tilde{\sigma}_{k-n} \left(\frac{\partial u}{\partial \zeta} \right)_n \right\rangle_{L^2(\Omega_{2D})} = \left\langle v_k, \tilde{f}_k \right\rangle_{L^2(\Omega_{2D})} \quad \forall v_k \end{array} \right.$$

hp finite element method

A Self-Adaptive Goal-Oriented *hp*-FEM

Optimal 2D Grid (TCRT Problem)



We vary locally the element size h and the polynomial order of approximation p throughout the grid.

Optimal grids are **automatically generated** by the computer.

The self-adaptive goal-oriented *hp*-FEM provides **exponential convergence** rates in terms of the CPU time vs. the error in a user prescribed quantity of interest.

Fourier finite element method

2D Finite Elements + 1D Fourier

3D Problem (using a Fourier Finite Element Method):

- $H(\text{curl})$ (**Nedelec elements**) for the meridian components ($E_{\rho,z}$), and
- H^1 (**Lagrange elements**) for the azimuthal component (E_ϕ).

2.5D Problem (using a Fourier Finite Element Method):

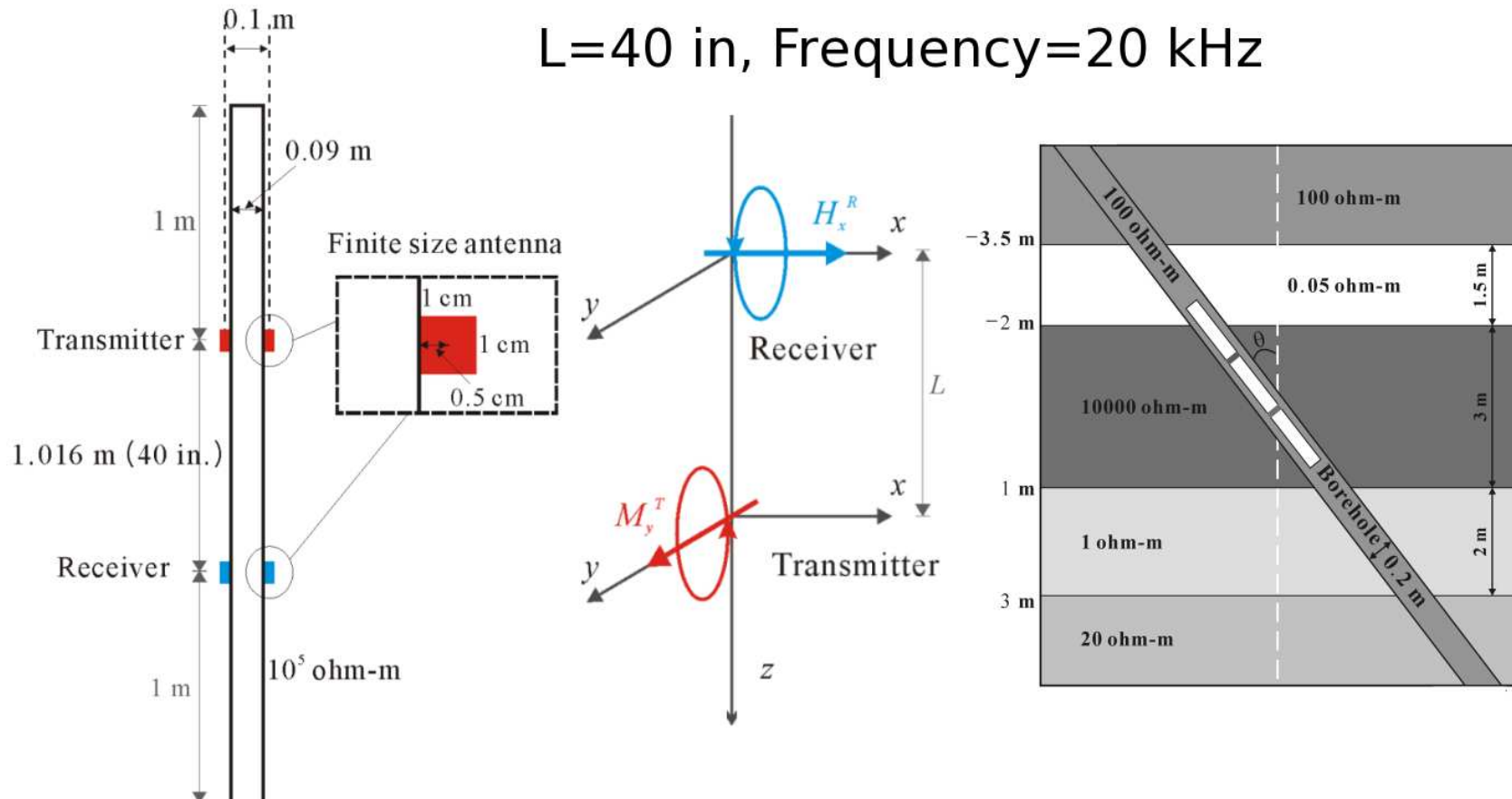
- $H(\text{curl})$ (**Nedelec elements**) for the meridian components ($E_{\rho,z}$), and
- H^1 (**Lagrange elements**) for the azimuthal component (E_ϕ).

2D Problem:

- $H(\text{curl})$ (**Nedelec elements**) in terms of the meridian components ($E_{\rho,z}$),
or
- H^1 (**Lagrange elements**) in terms of the azimuthal component (E_ϕ).

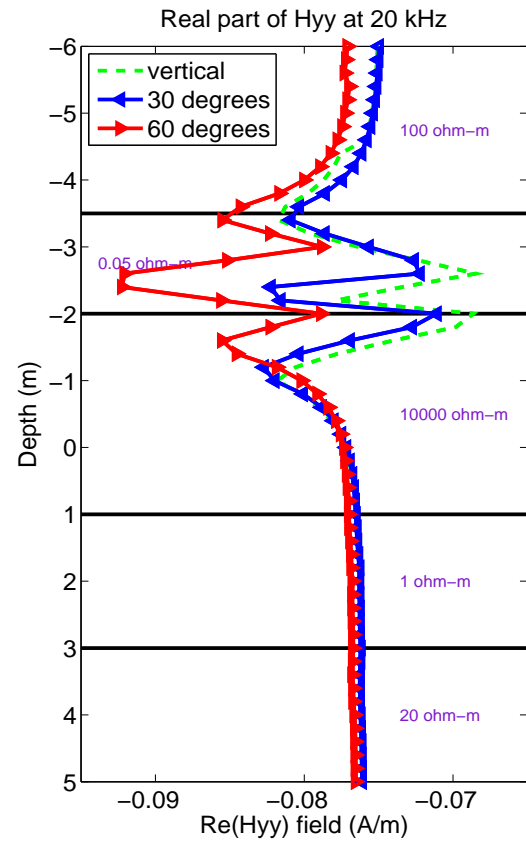
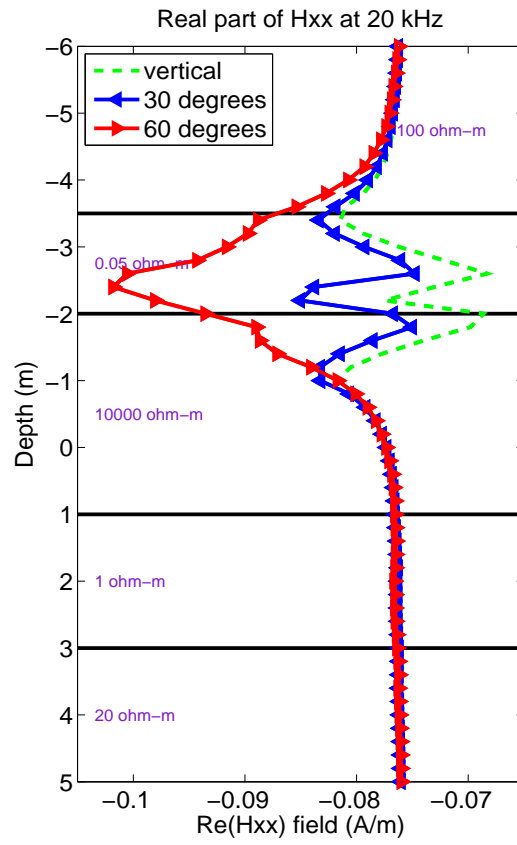
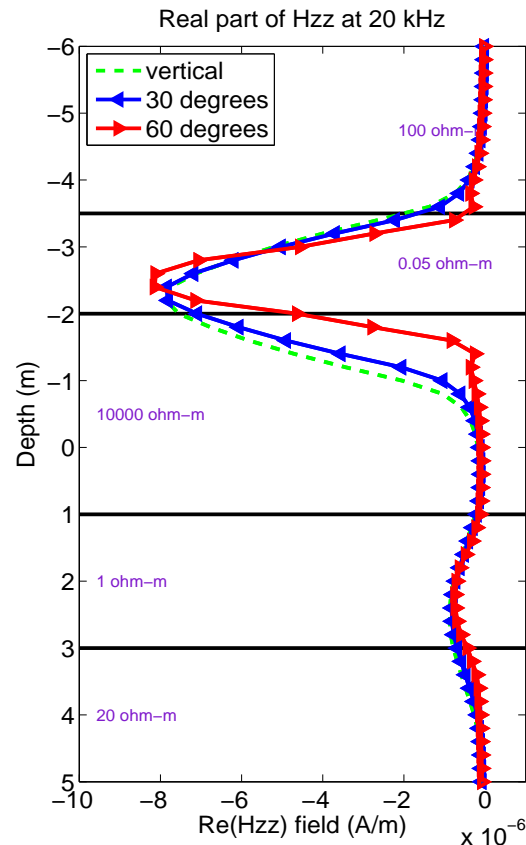
Logging electromagnetic applications

Tri-Axial Induction Tool



logging electromagnetic applications

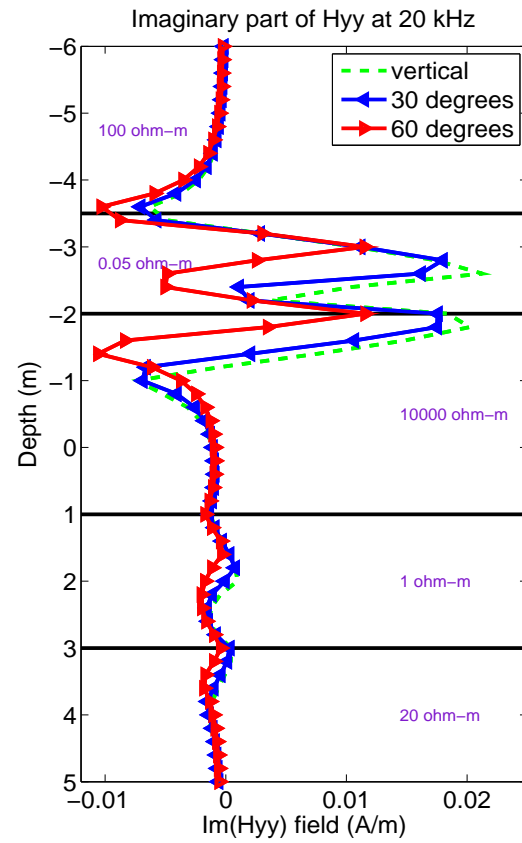
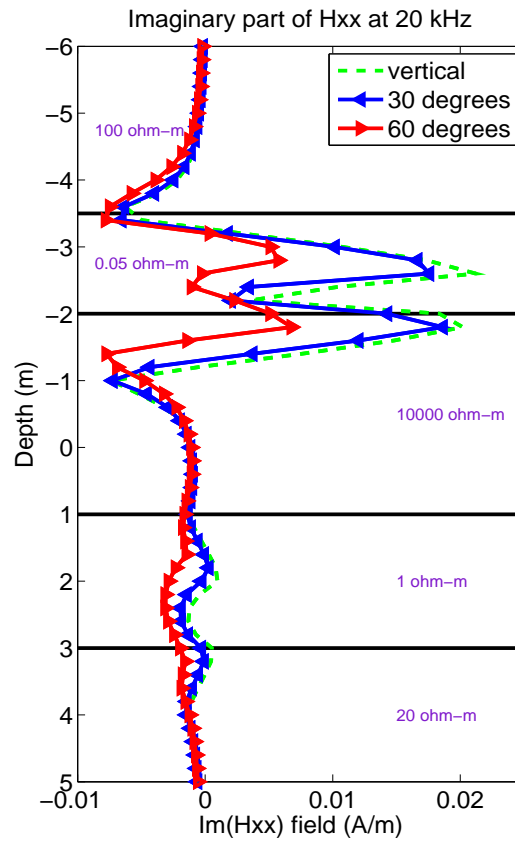
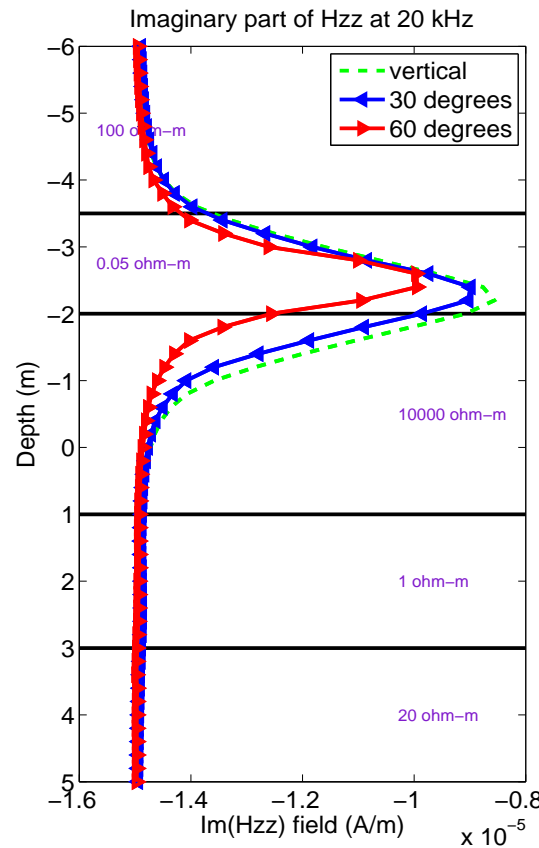
Tri-Axial Induction Tools in Deviated Wells (0, 30, and 60 degrees)



Triaxial tools are more sensitive to dip angle effects

logging electromagnetic applications

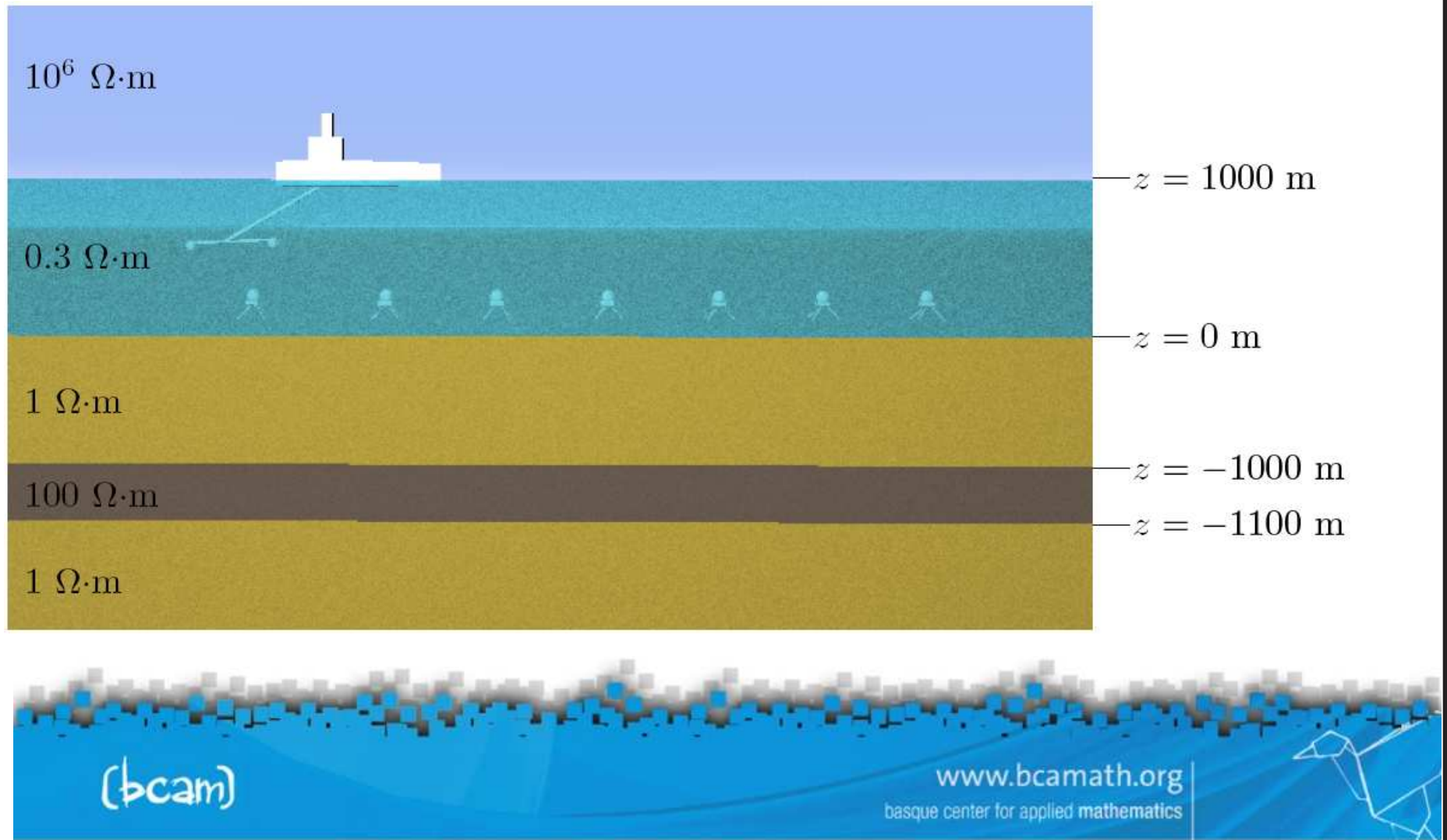
Tri-Axial Induction Tools in Deviated Wells (0, 30, and 60 degrees)



Triaxial tools are more sensitive to dip angle effects

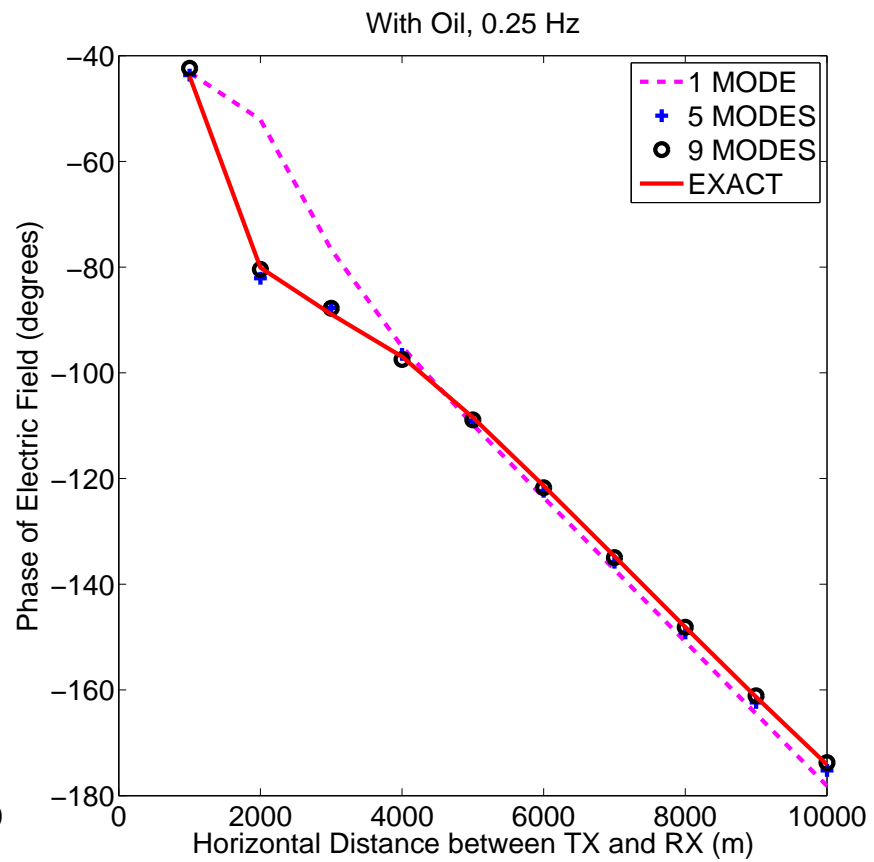
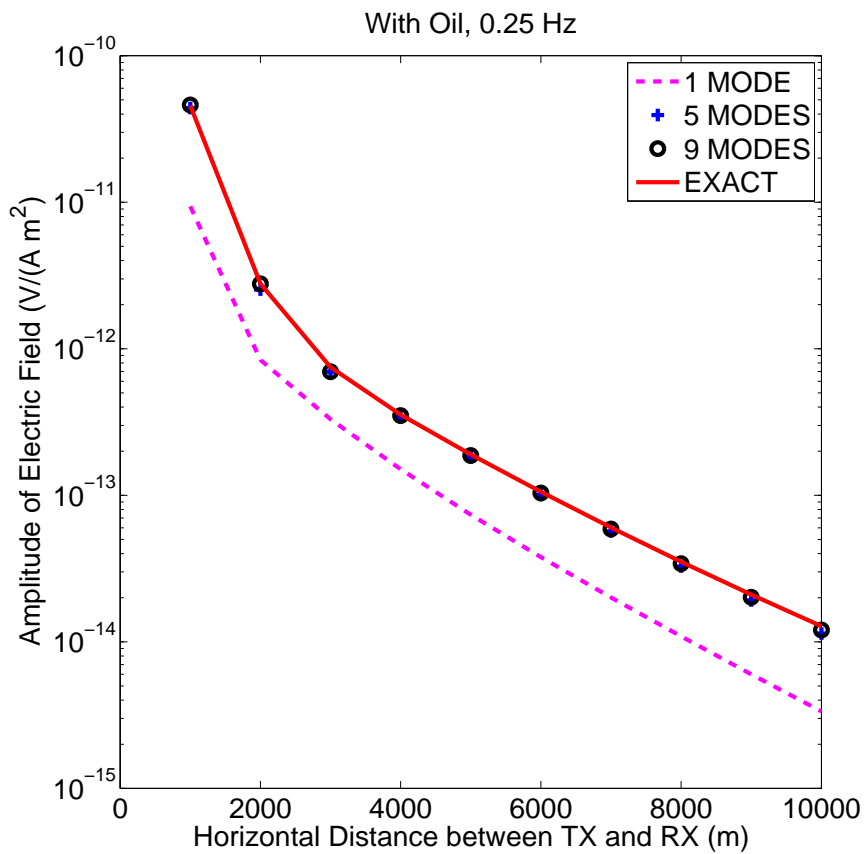
marine CSEM applications

Model Problem I: Marine CSEM Scenario with an Infinite Oil-Bearing Layer



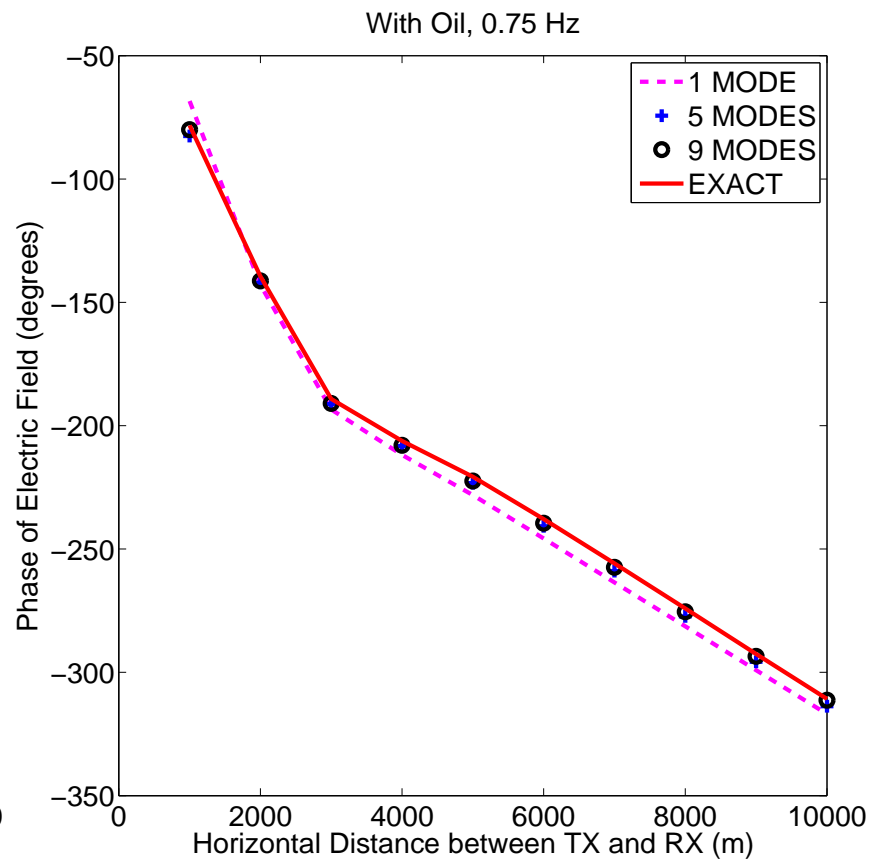
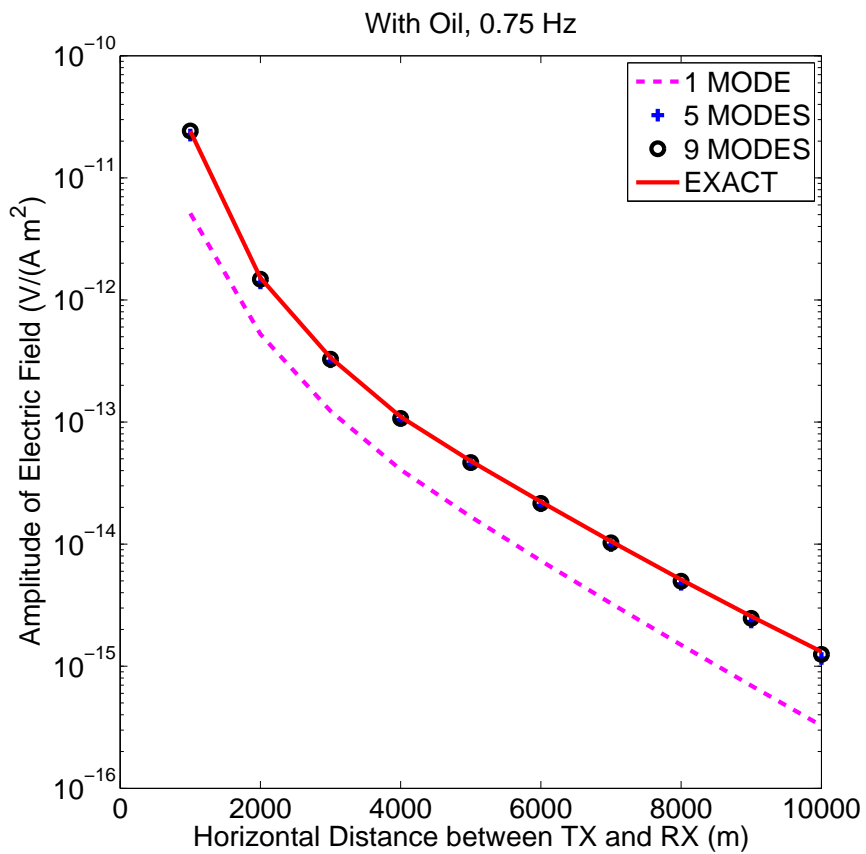
marine CSEM applications

Model Problem I: INFINITE OIL-BEARING LAYER — 0.25 Hz —



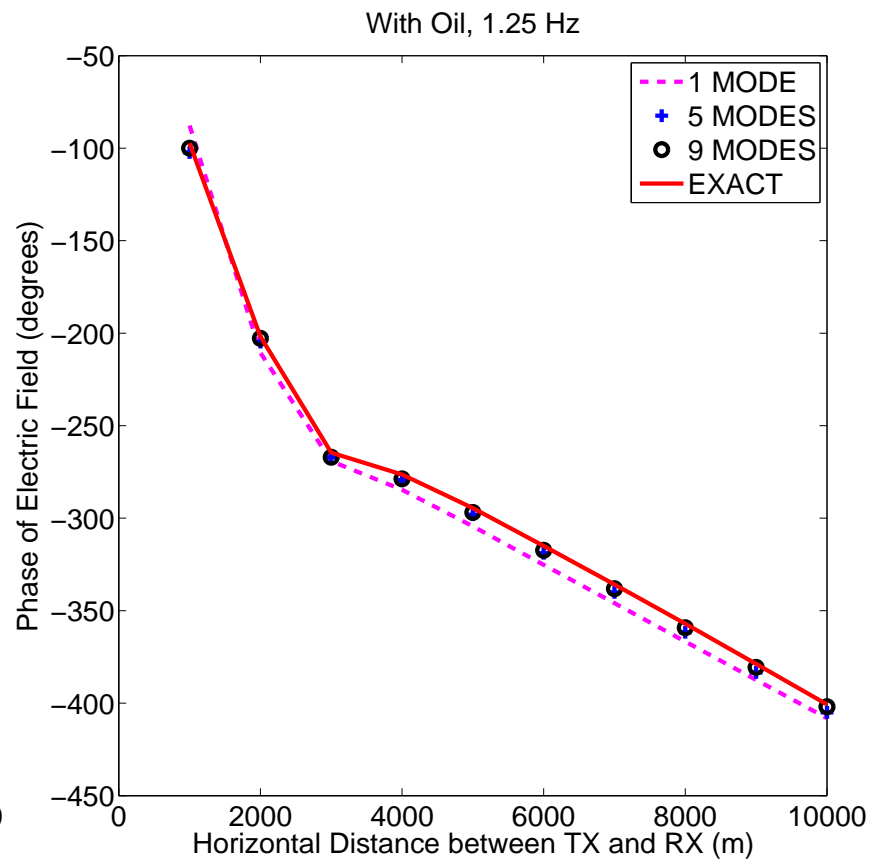
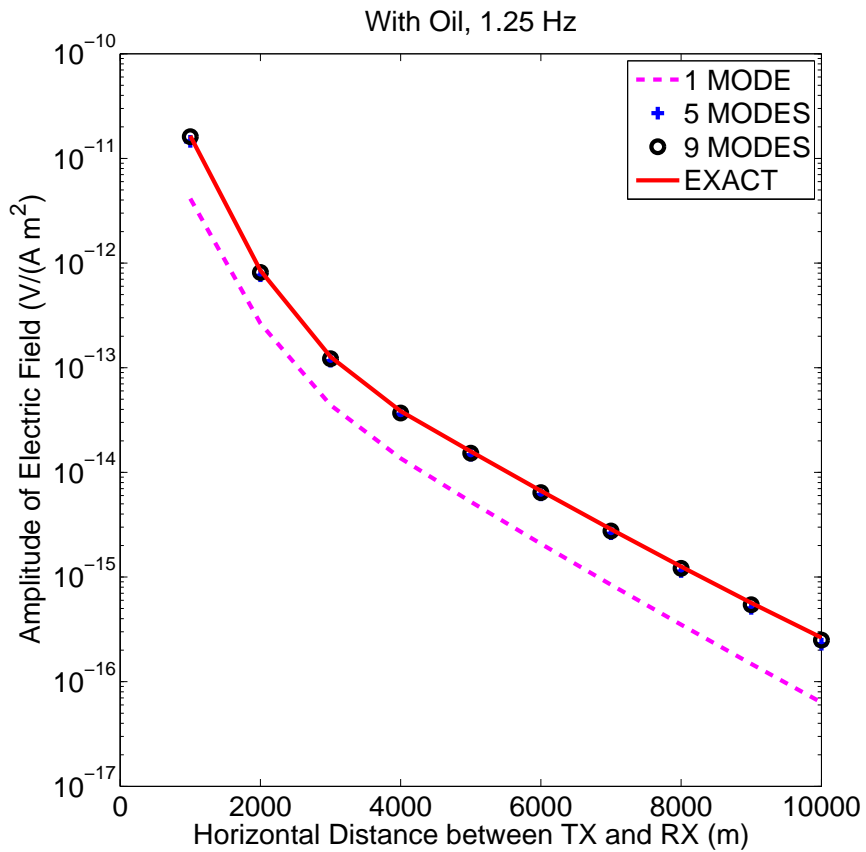
marine CSEM applications

Model Problem I: INFINITE OIL-BEARING LAYER — 0.75 Hz —



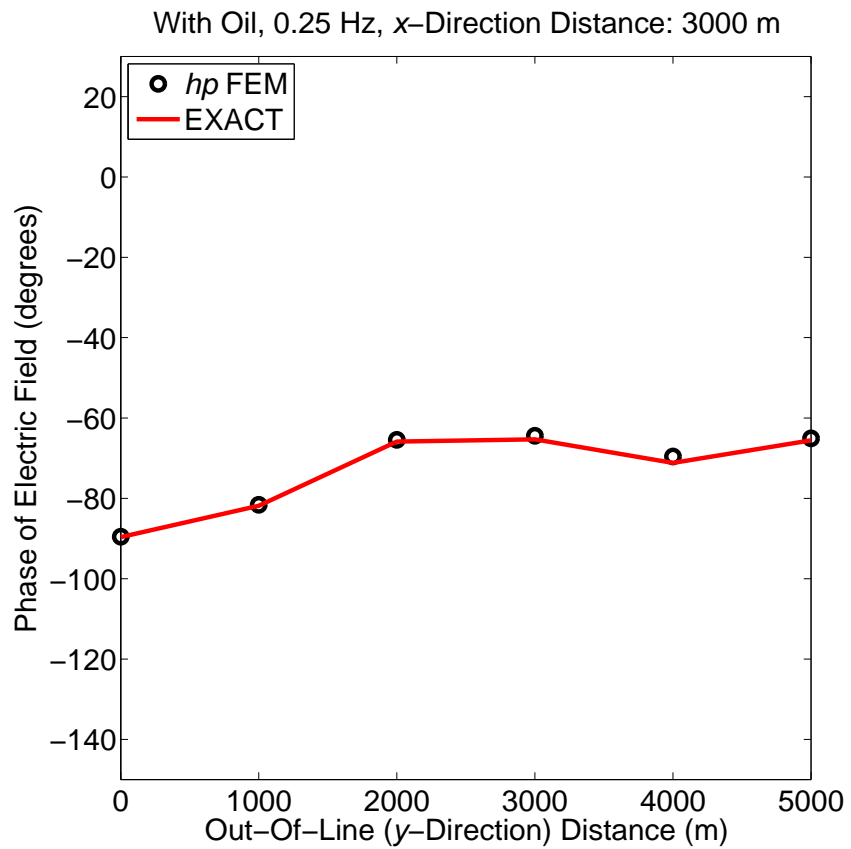
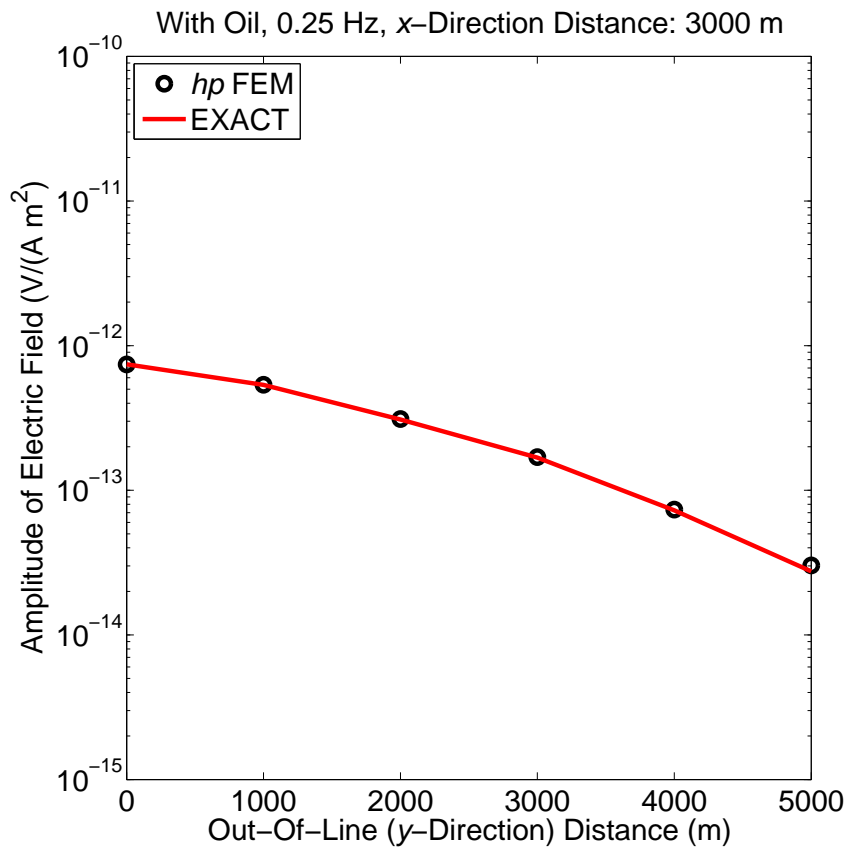
marine CSEM applications

Model Problem I: INFINITE OIL-BEARING LAYER — 1.25 Hz —



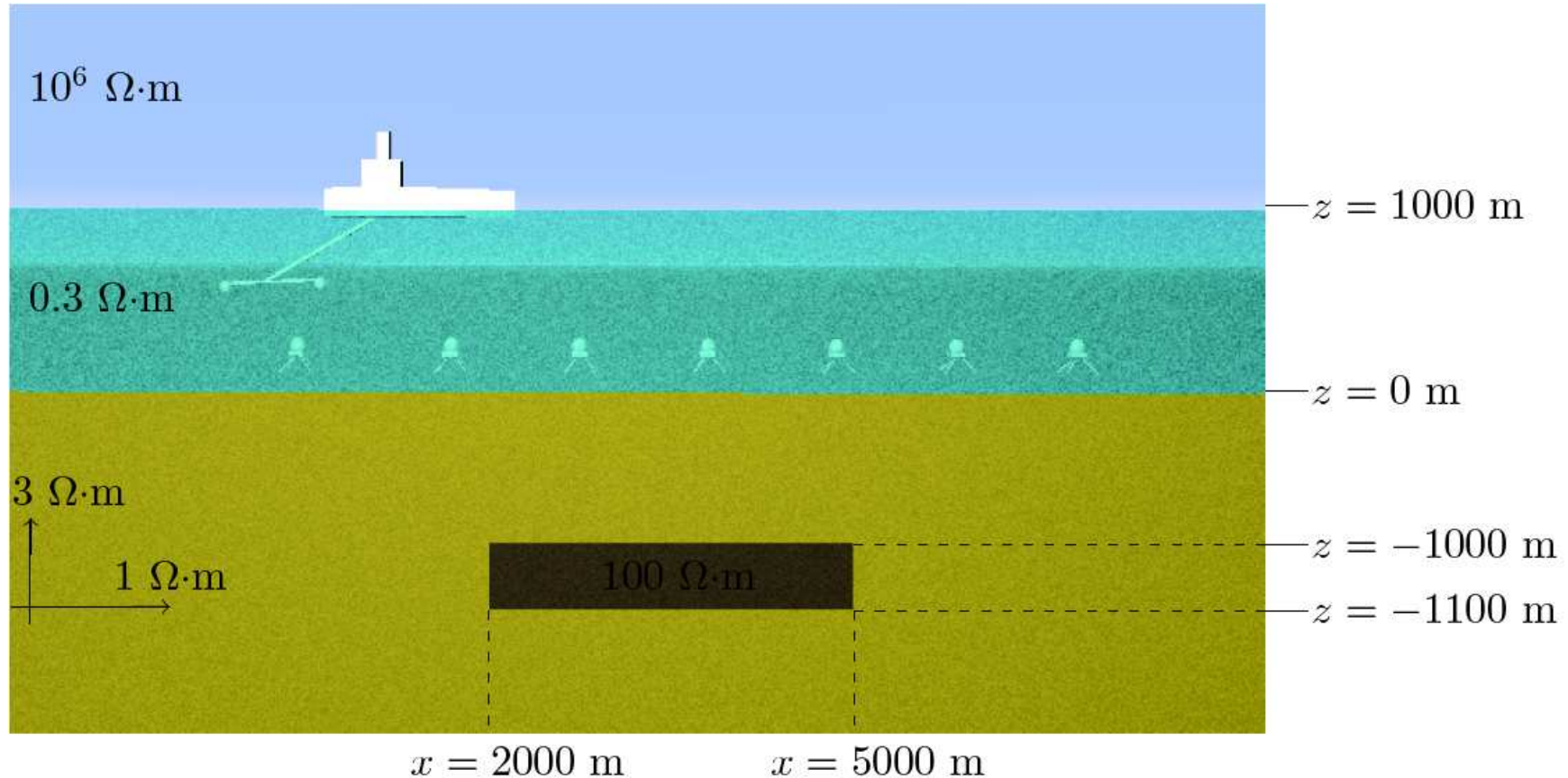
marine CSEM applications

Model Problem I: INFINITE OIL-BEARING LAYER — Out-of-line Receivers —

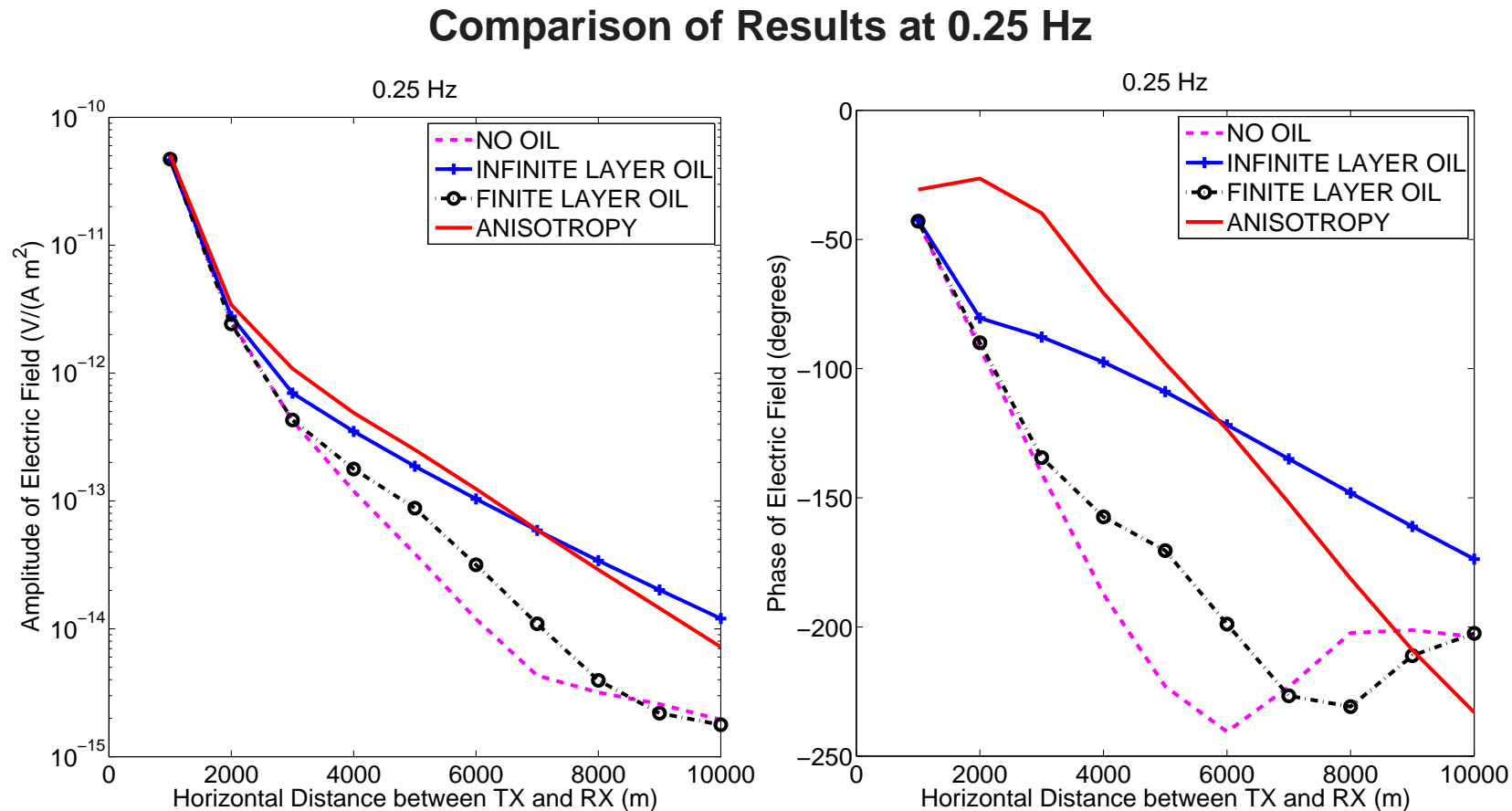


marine CSEM applications

Model Problem II: Marine CSEM Scenario with a Finite Oil-Bearing Layer



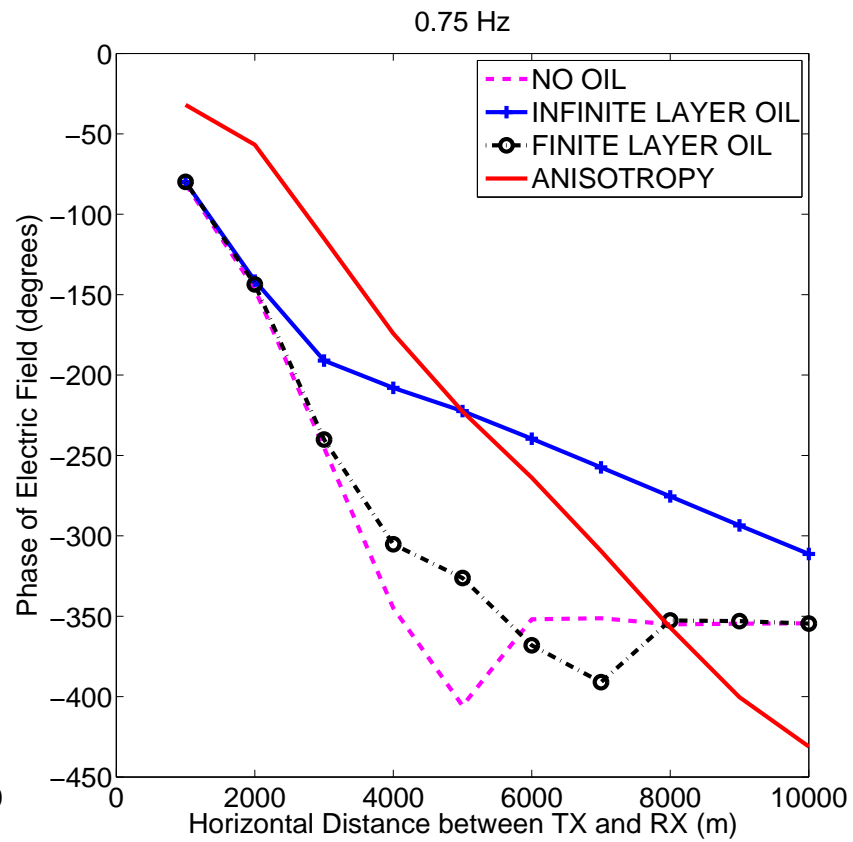
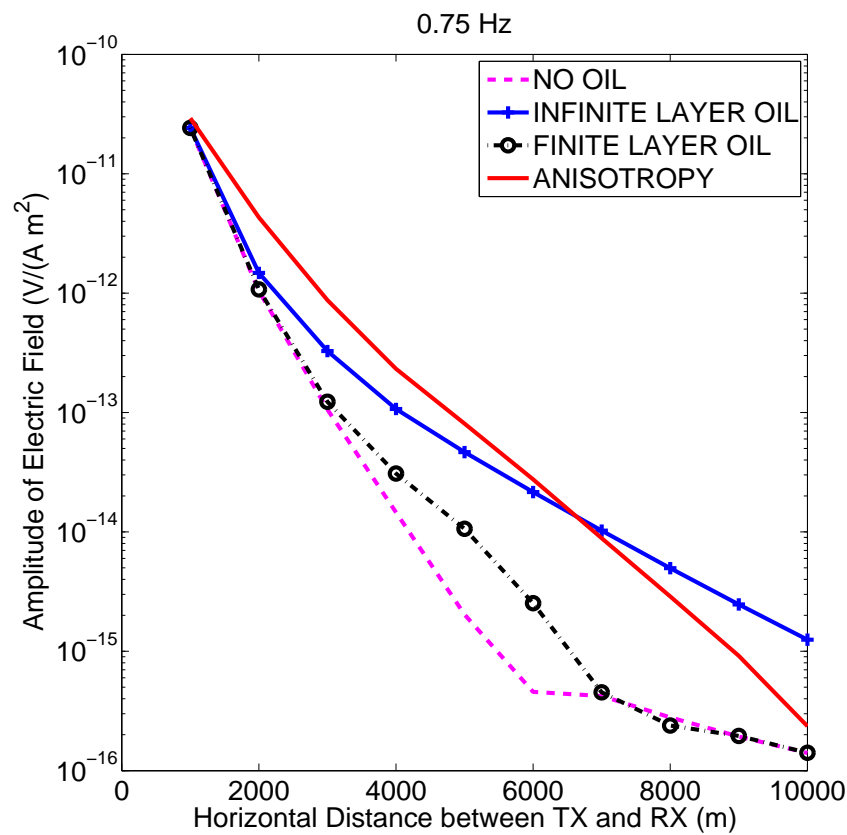
marine CSEM applications



The finite oil-bearing layer is clearly identified, and it is different from the solution for the infinite oil-bearing layer. To consider anisotropy is essential.

marine CSEM applications

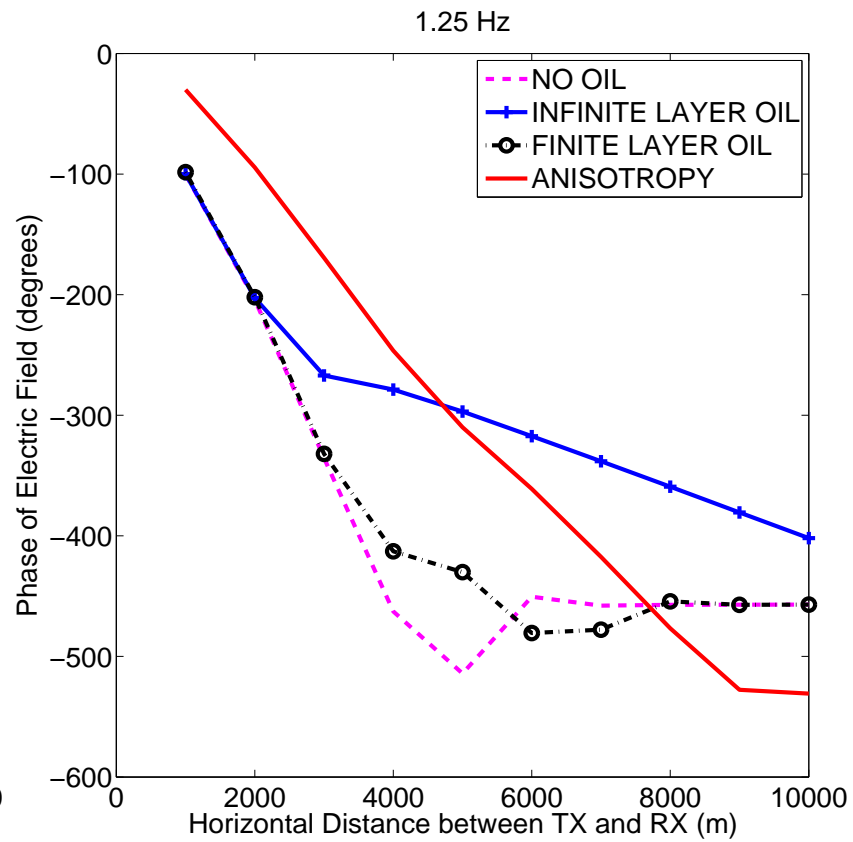
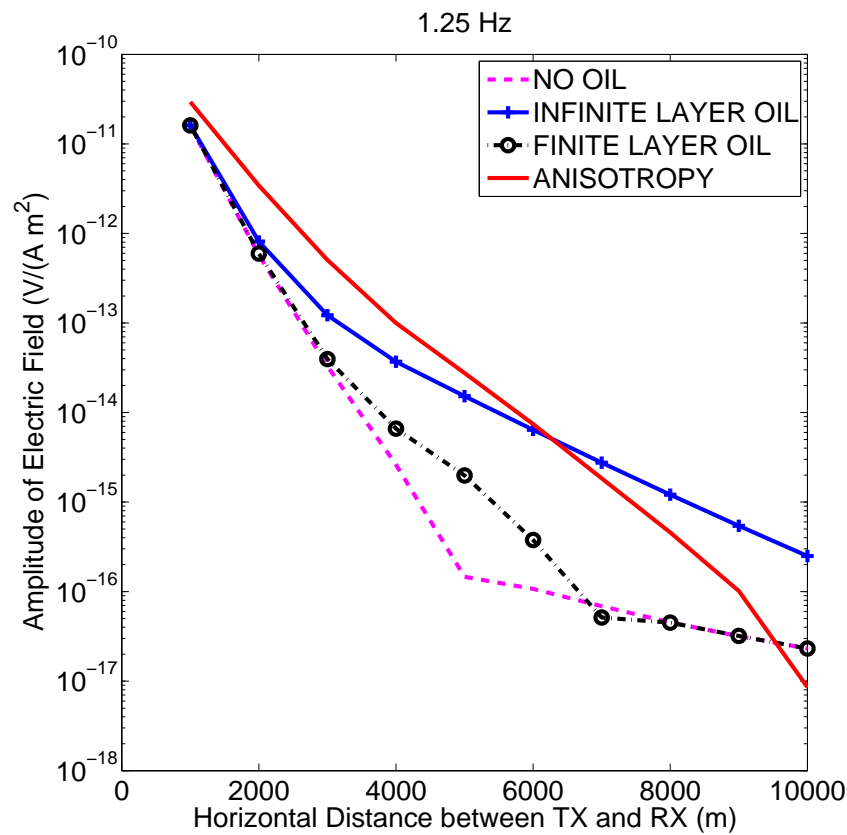
Comparison of Results at 0.75 Hz



As we increase the frequency, the effect of oil becomes more localized.

marine CSEM applications

Comparison of Results at 1.25 Hz



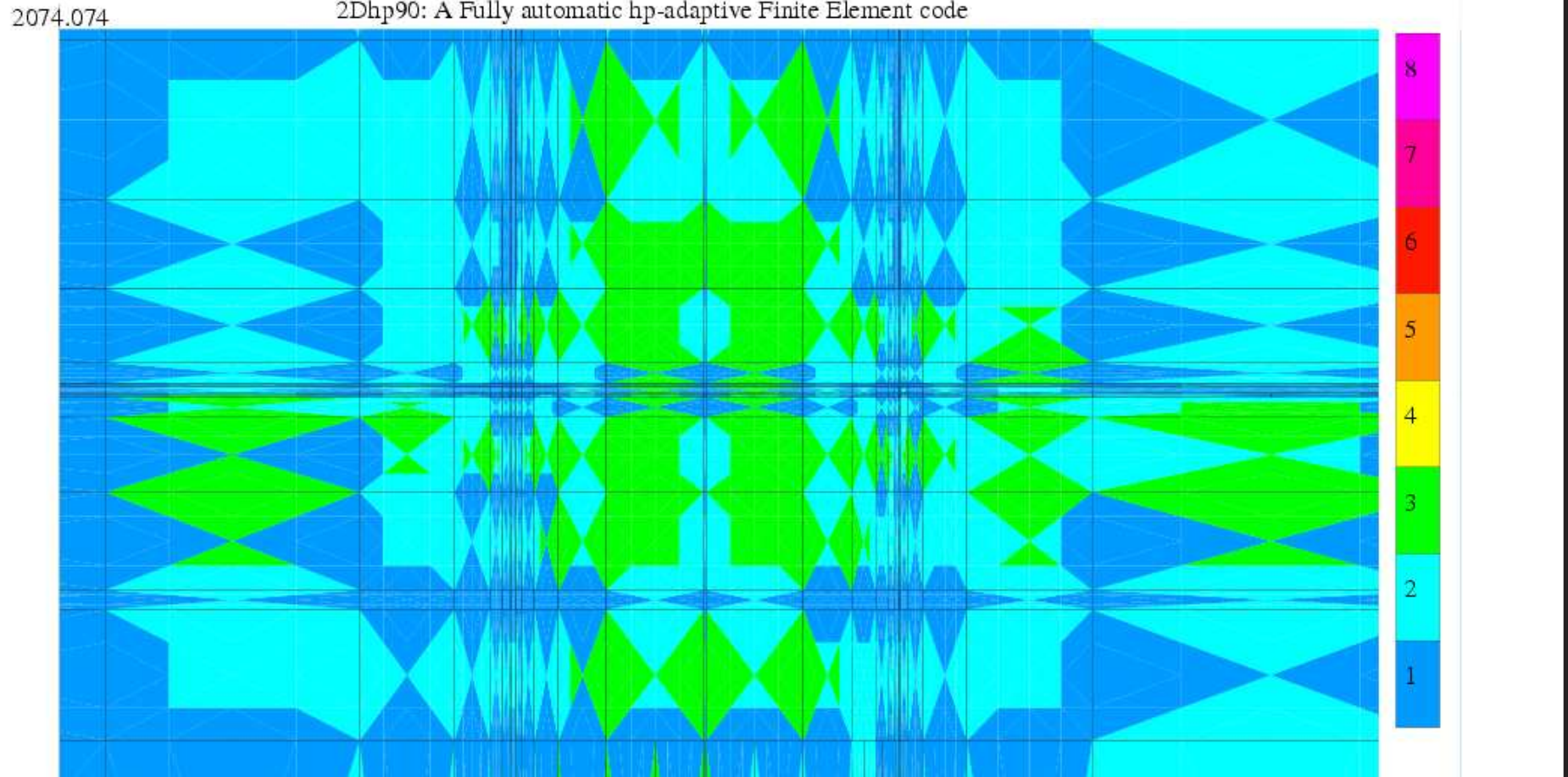
As we increase the frequency, the effect of oil becomes more localized.

marine CSEM applications

0.75 Hz (FINITE OIL-BERAING LAYER)

TX: $x = 0 \text{ m}$; RX: $x = 2000 \text{ m}$.

2Dhp90: A Fully automatic hp-adaptive Finite Element code

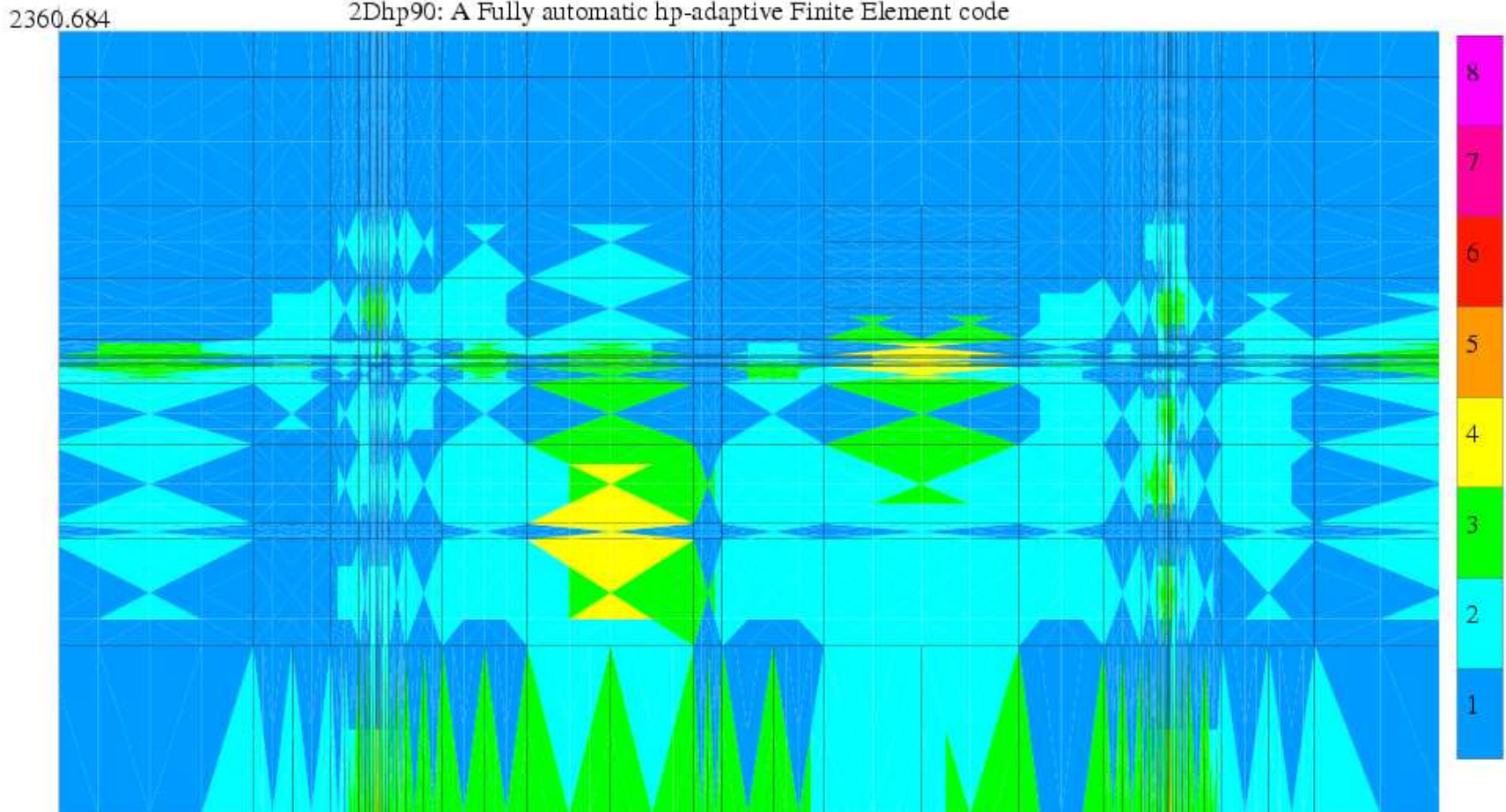


marine CSEM applications

0.75 Hz (FINITE OIL-BERAING LAYER)

TX: $x = 0 \text{ m}$; RX: $x = 5000 \text{ m}$.

2Dhp90: A Fully automatic hp-adaptive Finite Element code

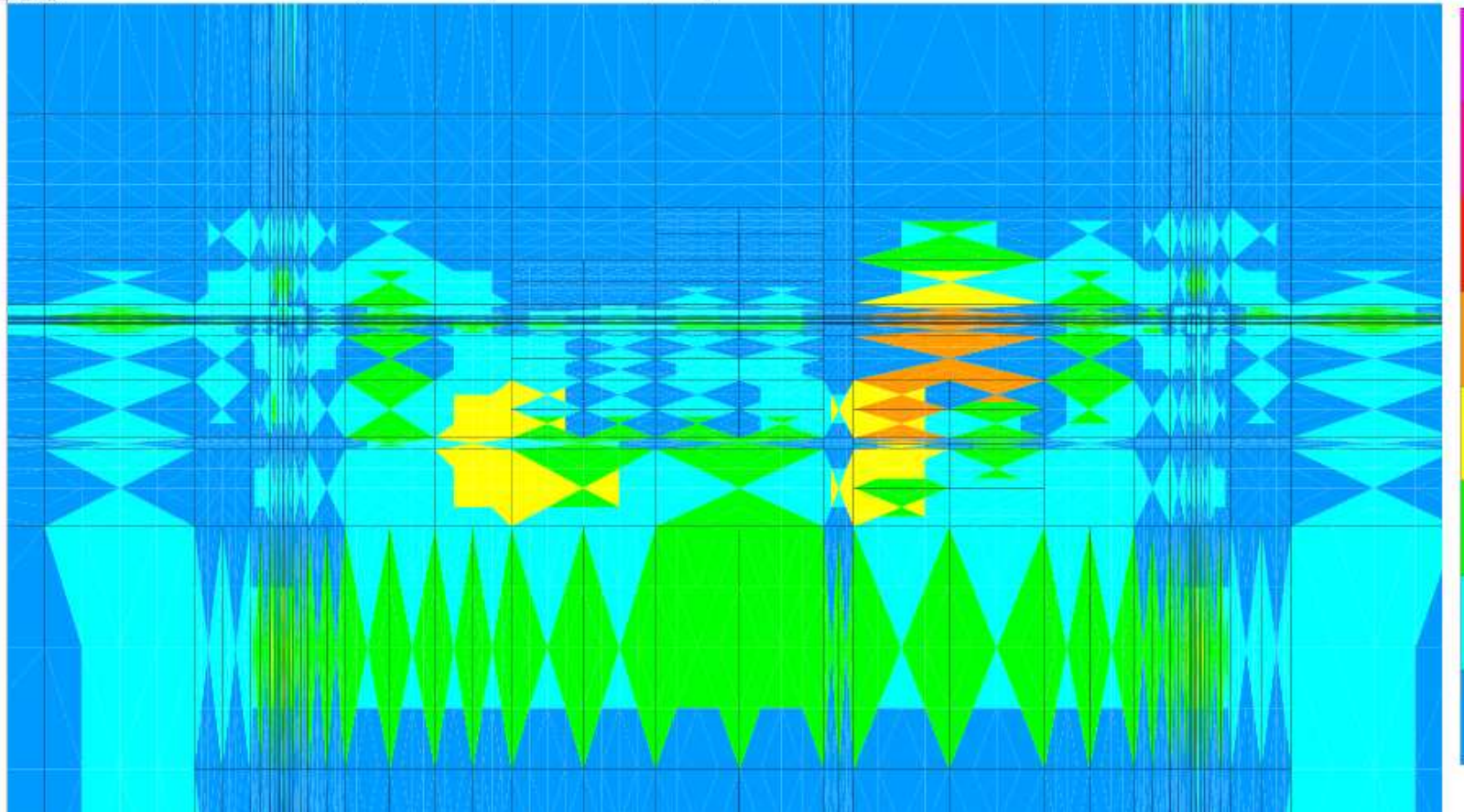


marine CSEM applications

0.75 Hz (FINITE OIL-BERAING LAYER)

TX: $x = 0 \text{ m}$; RX: $x = 8000 \text{ m}$.

3152.263
2Dhp90: A Fully automatic hp-adaptive Finite Element code



conclusions

- We have described an efficient numerical method based on a parallel self-adaptive goal-oriented hp refinement strategy and a Fourier-Finite-Element method.
- The method has been successfully used to simulate the acquisition of logging measurements and marine controlled-source electromagnetic (CSEM) problems.
- Our future research lines include: a) adaptivity for multiple goals, b) goal-oriented iterative solvers, and c) multiphysics applications.